Reduced protein diffusion rate by cytoskeleton in vegetative and polarized Dictyostelium cells

Potma, E.O; de Boeij, W.P.; Bosgraaf, L.; Roelofs, J; van Haastert, P. J. M.; Wiersma, D. A.

Published in:
Biophysical Journal

DOI:
10.1016/S0006-3495(01)75851-1

Publication date:
2001

Reduced Protein Diffusion Rate by Cytoskeleton in Vegetative and Polarized *Dictyostelium* Cells

Eric O. Potma,* Wim P. de Boeij,* Leonard Bosgraaf,† Jeroen Roelofs,† Peter J. M. van Haastert,† and Douwe A Wiersma*

*Ultrafast Laser and Spectroscopy Laboratory, Materials Science Centre, and †Groningen Biomolecular Sciences and Biotechnology Institute, University of Groningen, Nijenborgh 4, 9747 AG Groningen, The Netherlands

ABSTRACT Fluorescence recovery after photobleaching measurements with high spatial resolution are performed to elucidate the impact of the actin cytoskeleton on translational mobility of green fluorescent protein (GFP) in aqueous domains of *Dictyostelium discoideum* amoebae. In vegetative *Dictyostelium* cells, GFP molecules experience a 3.6-fold reduction of their translational mobility relative to dilute aqueous solutions. In disrupting the actin filamentous network using latrunculin-A, the intact actin cytoskeletal network is shown to contribute an effective viscosity of 1.36 cP, which accounts for 53% of the restrained molecular diffusion of GFP. The remaining 47% of hindered protein motions is ascribed to other mechanical barriers and the viscosity of the cell liquid. A direct correlation between the density of the actin network and its limiting action on protein diffusion is furthermore established from measurements under different osmotic conditions. In highly locomotive polarized cells, the obstructing effect of the actin filamentous network is seen to decline to 0.46 cP in the non-cortical regions of the cell. Our results indicate that the meshwork of actin filaments constitutes the primary mechanical barrier for protein diffusion and that any noticeable reorganization of the network is accompanied by altered intracellular protein mobility.

INTRODUCTION

The cell cytoplasm is a composite aqueous solution of multiple solutes, proteins, and electrolytes intersected by the multifaceted three-dimensional structure of the cytoskeleton. Mobility of molecular species like proteins within this complex environment is therefore suspected to deviate notably from mobility in dilute solutions (Luby-Phelps, 2000). The effective intracellular viscosity experienced by a target molecule is a complicated sum of the intrinsic viscosity of the liquid cell medium, nonspecific binding of probe molecule to macromolecules, and the mechanical barriers as imposed by the cytoskeletal network and organellar boundaries. Because the effective viscosity controls the rate of diffusion-limited enzymatic reaction and solute transport, an accurate determination of this physical property is of crucial importance in the understanding of the biochemical kinetics of the cell.

Recent studies have shown that the intracellular viscosity as sensed by macromolecules is two to five times higher than pure water (Luby-Phelps et al., 1986, 1987; Seksek et al., 1997). By comparing the rotational and translational diffusion properties of soluble intracellular green fluorescent protein (GFP) molecules it was deduced that mechanical obstructions constitute the primary barrier for protein mobility (Swaminathan et al., 1997). The filamentous structures of the cytoskeleton, collisions with macromolecular solutes, and confined motional freedom due to microcompartments will all affect protein diffusion. It is however unknown to what extent these different mechanisms contribute to the physical hindrance of protein mobility.

Actin is one of the major components that make up the cell cytoskeleton. In eukaryotic cells, actin is found at high concentrations of ~4 mg/ml from which half is polymerized into filamentous microstructures (Bray and Thomas, 1975). Filaments of actin play a key role in the maintenance of cell shape and are prominently involved in cytokinesis, organelle transport, and cell locomotion (Cooper, 1991; Fishkind and Wang, 1995). Previous studies have shown that the actin network, which results from different degrees of cross-linking between filaments, slows down the long-time diffusion rate of long-chain dextrans in neurons (Popov and Po, 1992). In the typical mammalian cell, the three-dimensional actin cytoskeleton is suspected to constitute an important mechanical barrier for protein diffusion as well. Furthermore, given the dynamic redistribution of the actin filamentous network depending on extracellular and intracellular conditions, it is likely that its influence on protein motional freedom will vary as well.

Although it is generally believed that the actin cytoskeletal network exerts influence on the motional freedom of cellular constituents, no quantitative measurements have been reported on its actual effect on proteins. In this contribution we focus on the impediment of short-time protein diffusion enforced by the actin filamentous meshwork in *Dictyostelium discoideum* amoebae. The cell biology of *D. discoideum* resembles that of ameboid mammalian cells, which makes *Dictyostelium* a good model system for studying protein diffusion (Spudich, 1987). The dynamics and distribution of the actin filaments in *Dictyostelium* cells has been extensively studied. Various functional mechanisms bring about a rigorous redistribution of filamentous actin.

Received for publication 8 March 2001 and in final form 26 June 2001.

Address reprint requests to Dr. Peter J. M. van Haastert, Groningen Biomolecular Sciences and Biotechnology Institute, University of Groningen, Nijenborgh 4, 9747 AG Groningen, The Netherlands. Tel.: 31-50-363-4172; Fax: 31-50-363-4165; E-mail: P.J.M.Haastert@chem.rug.nl.

0006-3495/01/10/2010/10 $2.00

Under hypertonic conditions, for instance, an osmo-induced protection mechanism is activated in which a sizeable rearrangement of the cytoskeletal meshwork is involved (Kuwayama et al., 1996; Zischka et al., 1999). Hereby a notable stacking of polymerized actin was observed near the cellular rim, which is accompanied by a relative depletion of the actin network density in the central region of the cell. Also, in highly motile and polarized *Dictyostelium* cells, actin filaments are seen to accumulate near the leading and retracting edges of the cell (Yumura and Fukui, 1998; Ming Pang et al., 1998; Novak and Titus, 1997). A particular advantage of using *D. discoideum* cells is that these different organizations of the actin network can be fairly controlled under laboratory conditions. Here we employ fluorescence recovery after photobleaching (FRAP) measurements to elucidate the short-time diffusion of GFP in cytoplasmic regions of the cell conditional on the distribution of filamentous actin in vegetative and polarized cells.

Because the differences in protein mobility as a function of the arrangement of actin networks are expected to bring about only subtle changes in the photobleaching profiles, a sensitive detection method is a prerequisite. We have utilized a confocal detection scheme to monitor more sensitively the recovery kinetics near the focal volume, which facilitates the measurement in small cells like *Dictyostelium*. In addition, we have analyzed our experimental data with a detailed model that allows extracting GFP diffusion constants from the measurements with great accuracy. Our results indicate that translational motions of protein-sized molecules are severely limited by the polymerized actin meshwork. Moreover, a direct correlation between the dispersion of actin filaments and protein mobility is established.

MATERIALS AND METHODS

Chemicals

Soluble enhanced GFP (EGFP) was purchased from Clontech (Palo Alto, CA). Fresh solutions of 0.4 μM fluorescent protein in pH 8.0 Tris-HCl buffer were prepared before experiments. Latrunculin-A was bought from Molecular Probes (Eugene, OR) and stored as a stock solution of 0.1 mM in DMSO.

Cell culturing and handling

Wild-type *D. discoideum* cells of strain AX3 were transfected with plasmid constructs containing the gene for GFP-S65T and a blasticidin or neomycin resistance cassette. Cells were cultivated in HG5 medium in petri dishes in the presence of 10 μg/ml blasticidin or neomycin, depending on the resistance marker. For photobleaching experiments, cells were harvested at a density of $\sim 10^6$ cells per ml and washed twice with phosphate buffer (17 mM, pH 6.4). A 100-μl droplet of cell suspension in buffer, containing $\sim 10^5$ cells, was spread on a coverglass for microscopic examination. For measurements on polarized amoebae, cells on coverglasses were suspended in a non-nutrient buffer and incubated in a moisturized petri dish. After $\sim$5 h, cells started to polarize spontaneously to form cell aggregates. During this stage, FRAP measurements were performed on polarized cells over a time span of $\sim$4 h. All experiments were conducted at room temperature.

Instrumentation

Confocal spot photobleaching recovery measurements were performed on a modified microscope system (Zeiss Axiovert S100TV, Oberkochen, Germany). The 488-nm radiation of an argon ion laser is split by a cube beam splitter to generate a pump beam for photobleaching and a much weaker probe beam to monitor the subsequent fluorescence recovery. After passage through an acoustic optic modulator (Soro Electro-optics, Boulogne, France) the diffracted part of the pump beam is collinearly aligned with the probe beam. Both beams are expanded such as to totally overfill the back aperture of the microscope objective (Zeiss Neofluar, $\times$40, 0.75 NA, Oberkochen, Germany). Optical density filters are used to limit the probe power to 1 μW whereas the average power of the pump amounts to less than 1.0 mW upon entrance of the microscope. A bleach pulse duration of 100 μs is used in the experiments. Fluorescence is collected in the epi-direction, separated from the excitation light by a 500-nm dichroic mirror (Chroma, Brattleboro, VT) and detected through a confocal pinhole by an avalanche photodiode (EG&G, Vandreuil, Canada). The overwhelming signal during the bleaching period is suppressed by gating the output of the photodetector. FRAP signals are sampled by a multichannel scaler (Stanford Research Systems, Sunnyvale, CA). Additionally, the sample is illuminated in bright field with dim light from a halogen lamp that has passed through a 450-nm interference filter. This radiation is isolated from both the 488-nm laser light and emitted fluorescence using a dichroic mirror of 470 nm and guided to a CCD camera (Hamamatsu Photonics, Hamamatsu City, Japan) that is placed in the conjugated image plane of the microscope objective. The present geometry allows the realization of photobleaching experiments while the CCD camera simultaneously visualizes the cells. Sample position is controlled by a piezo-translation stage (PI).

Microscope calibration

Obtaining quantitative diffusion parameters from the experimental data requires an accurate determination of the focal volume of the microscope. By scanning fluorescent microspheres (20 nm, Molecular Probes, Eugene, OR) through focus, a confocal lateral resolution of 0.26 μm and an axial resolution of 1.32 μm are determined. The three-dimensional focal intensity distribution of the objective lens is described excellently by a diffraction-limited point-spread function that corresponds to an effective numerical aperture (NA) of 0.65. The latter value is used to simulate the diffraction-limited focal volume in analyzing the experimentally obtained FRAP data.

Relative to the non-confocal geometry, the confocal probing volume is more confined, especially in the axial direction. As a consequence, a confocal detection scheme is much more sensitive to the recovery kinetics in the immediate vicinity of the focal spot and less sensitive to regions away from the principal axis. As long as the volume probed falls well within a region homogeneously filled with fluorophores, the confocal method can be applied to study molecular diffusion without making stringent assumptions concerning the geometrical organization of the sample. In the spot photobleaching experiments with confocal detection, a bleach depth of 25% is realized using the excitation conditions as described above. We verified experimentally that for non-confocal detected FRAP, a similar bleach depth is obtained when the pump power is almost four times increased.

Estimates of the volume of *D. discoideum* cells are obtained from three-dimensional confocal images. Taking into account the confocal resolution of the microscope, effective contour functions were determined from the data stack and numerically integrated using home-written software. Highly irregular cells and cells exhibiting multiple pseudopodia were

excluded from the analysis to minimize experimental uncertainty. Under the different conditions examined, cell volumes were determined from an average of the volumes of 15 individual cells.

Data acquisition

Computer software controls the repetition rate and time window of the experiment. Measurements are triggered by a computer-generated pulse. Fluorescence signals are monitored before and after the bleach pulse. In the present experiments, signals are recorded in timeframes of 50 ms, 200 ms, or 2 s. Data are binned into 1024 points and stored in the computer. Up to 10 FRAP traces are taken per cell at different intracellular positions and subsequently averaged. In polarized cells, a FRAP recording is initiated every second while the cell migrates through the focal volume. The position of the cell with respect to the focal spot is monitored at every instant on the CCD camera. Individual photobleaching traces are subdivided into three categories: the front side, the middle part, and the rear side of the cell. Average curves are generated in each of these categories. Measurements in which the probed volume is not entirely filled by the cell body are rejected from the analysis. Severe underfilling of the focal volume leads to an underestimation of the diffusion constant (Blonk et al., 1993; Brown et al., 1999). These situations are encountered when the focal spot is positioned in the immediate vicinity of the cell boundaries. For these reasons, molecular diffusion in regions close to the plasma membrane is not considered in this study.

Data analysis

To extract diffusion coefficients from the measurements with a high accuracy we use a model that solves the diffusion equation involved in an exact manner. In the following, we briefly explain the fundamentals of our approach. In photobleaching experiments, an intense laser pulse bleaches irreversibly part of the fluorophores in the illumination volume. The spatially varying concentration of active fluorescent molecules immediately after the bleaching event is given by (Axelrod et al., 1996):

$$c(r, z, t = 0) = c_0 \exp[-\alpha T I(r, z)] \tag{1}$$

The lateral and axial coordinates are indexed by r and z, respectively, α is a bleaching parameter, T refers to the duration of the bleaching pulse, and $I(r, z)$ corresponds to the point-spread function of the microscope objective. Due to translational diffusion of the fluorescent proteins the concentration pattern evolves in time. The concentration at later times is governed by the diffusion equation:

$$\frac{\partial c(r, z, t)}{\partial t} = D\nabla^2 c(r, z, t) \tag{2}$$

The molecular diffusion coefficient is written here as D. Equation 2 may be transformed to the spatial frequency domain using a Fourier-Hankel transformation. The result of this operation can be expressed as:

$$\frac{\partial c(\rho, \omega, t)}{\partial t} = D(-4\pi\rho^2 - \omega^2)c(\rho, \omega, t), \tag{3}$$

where ρ and ω are the spatial frequency analogs of the lateral and axial coordinates, respectively. The solution of Eq. 3 is expressed as:

$$c(\rho, \omega, t) = c(\rho, \omega, t = 0)\exp[-4\pi\rho^2 Dt]\exp[-\omega^2 Dt], \tag{4}$$

where $c(\rho, \omega, t = 0)$ is the Fourier-Hankel transformed expression of Eq. 1. The evolution of the concentration profile can be followed in time by recording the fluorescence emission of the active fluorophores under the low-excitation conditions of the probe beam. The monitored fluorescence is finally given by:

$$F(t) = 2\pi \int\int I(\rho, \omega)c(\rho, \omega, t)\rho d\rho d\omega, \tag{5}$$

where $I(\rho, \omega)$ corresponds to the confocal point-spread function of the objective lens. Equation 5 is numerically integrated and fitted to the experimentally determined FRAP traces.

Modeling of the intracellular diffusion

Molecular diffusion in solution generally depends on temperature, viscosity of the medium, and the geometrical details of the diffusing entity. According to the Stokes-Einstein relation the diffusion coefficient can be expressed as:

$$D = \frac{KT}{6\pi a\eta} \tag{6}$$

where K denotes Boltzmann's constant, T stands for temperature, and a relates to the hydrodynamic radius of the molecule. Diffusion is seen to be inversely proportional to the viscosity η of the solvent. In cells, translational motions of a GFP-sized molecule are influenced by both the physical properties of the cell liquid and by mechanical obstructions. The translational motions of GFP in the cytoskeletal network are suspected to be determined by percolation rather than by the flexibility of the network (Johansson and Löfroth, 1993). Hence, the viscoelasticity of the actin filaments is assumed to be irrelevant. A similar rationale applies for interactions of the GFP molecule with other mechanical boundaries. We may therefore define an effective intracellular viscosity as:

$$\eta_{\text{eff}} = \eta_{\text{med}} + \kappa_{\text{actin}} + \kappa_{\text{other}} \tag{7}$$

Here we separate the solvent-like effect of the cell medium (η_{med}) from the obstructing activity of mechanical barriers (κ). In the model of an ideal solvent, the viscosity of the cell medium shows a linear dependence on the intracellular molecular concentration and, consequently, on any relative change of the total cell volume V_0:

$$\eta_{\text{med}} = \eta_0 + cV_0/V, \tag{8}$$

where η_0 is the viscosity of pure water (η_0 = 1.0 at 293 K) and c is a constant. Thus, in our simplified description, the hindered motion of the GFP molecules administered by actin filaments is treated on an equal basis with other mechanical impediments and more solvent-like induced restricted motions. As a result, the data can be interpreted in terms of a single diffusion coefficient D. Our description of the restrained GFP mobility follows from the more general expressions derived by Brinkman describing the hindered motions of particles in hydrogels (Brinkman, 1947; Johnson et al., 1996). When it is assumed that the cell liquid behaves as a dilute aqueous solution at room temperature, the following relation holds:

$$\frac{D_{\text{cell}}}{D_0} = \frac{1}{1 + \kappa}, \tag{9}$$

where D_0 refers to unrestricted molecular diffusion in dilute solution. Equation 9 relates to the Brinkman result. In the present study we use Eqs. 7 and 8 to effectively mimic the influence of both the cell medium and the mechanical interactions on protein diffusion.

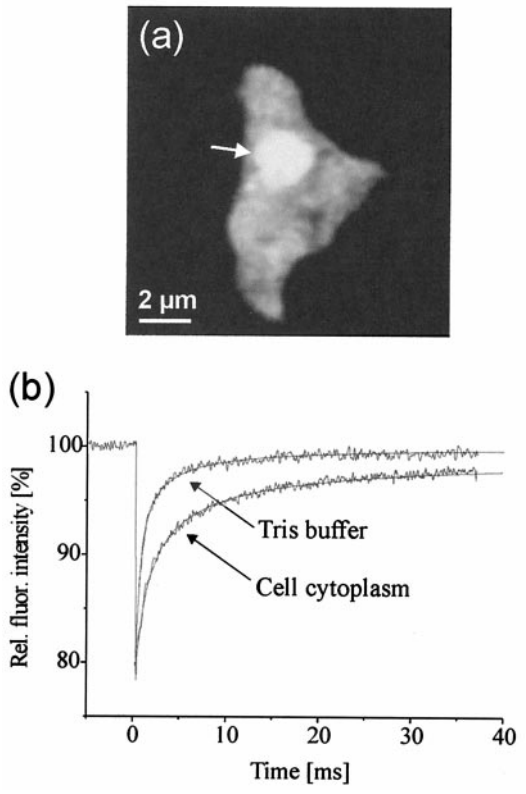

FIGURE 1 Photobleaching experiments of GFP in *D. discoideum*. (*a*) Expression of soluble GFP results in a homogeneous staining of the cytoplasm and aqueous lumen of certain organelles such as the nucleus (*arrow*). (*b*) Fluorescence recovery traces after photobleaching GFP in dilute solution (0.4 μM in Tris-HCl, pH 8) and in cells. In the aqueous buffer, a single-component diffusion coefficient of $D = 87 \pm 3$ $\mu m^2/s$ was found from a fit to the recovery profile. In cytoplasmic domains of the cell, a diffusion constant of 24 ± 2 ($n = 46$) was determined.

RESULTS

Translational protein diffusion in vegetative *Dictyostelium* cells

The fluorescence recovery of EGFP in Tris-HCl buffer after photobleaching is shown in Fig. 1 *a*. Due to diffusive translational motions of the protein, the irreversibly bleached fraction is rapidly replaced by neighboring active fluorescent proteins. Within 1 s, the pre-bleach fluorescence level is retained completely. When the focusing conditions are changed, by utilizing either a 63×, 1.2W NA or a 20×, 0.5 NA objective for excitation, the recovery rate shows a dependence on the size of the bleaching spot in accordance with theory. A residual contribution from reversibly bleached EGFP molecules is not observed from the recorded profiles. In the concentration range 0.1–1.0 μM, the photobleaching curves follow identical profiles. The recovery kinetics is satisfactorily described by a diffusion coefficient of 87 $\mu m^2/s$, which fully corroborates previous studies (Swaminathan et al., 1997; Terry et al., 1995).

Dictyostelium cells expressing soluble GFP show a homogenous distribution of the fluorescent protein over the cellular cytoplasm (Fig. 1 *b*). Judging from the fluorescence signal levels, an intracellular GFP concentration of 0.2–1 μM is estimated. Most of the cells selected using blasticidine as a selection marker exhibit micron-sized spots that are characterized by a twofold increased fluorescence level. As verified with a 4,6-diamidino-2 phenylindole staining assay, these spots coincide with the nucleus (data not shown).

Compared with EGFP in solution, a much slower rate of fluorescence recovery is observed for soluble GFP in the cytoplasm of *Dictyostelium* cells. In addition, the amount of recovered fluorescence after 1 s has diminished with ~4% relative to pre-bleach signal levels. This observation indicates that a small fraction of the intracellular GFP molecules is immobile or, likewise, characterized by a diffusion constant that is a few orders of magnitude lower than the rapidly diffusing fraction. As identified by changing the size of the illumination volume, components reminiscent of reversible photobleaching are not interfering with the irreversible photobleaching recovery process in the cellular cytoplasm. A diffusion coefficient of 24 $\mu m^2/s$ is found from the intracellular recovery trace, which corresponds to a translational diffusion in the cytoplasm that is 3.6 times slower than in buffer solution. Comparable values of GFP diffusion have been reported in various types of mammalian cells (Swaminathan et al., 1997). In the cell nucleus, the GFP diffusion constant is determined to be 22 $\mu m^2/s$. Similar to the situation encountered in the cellular cytoplasm, a small immobile fraction of 4.0% is observed in the nucleus. The close resemblance of the diffusion constant in the cytoplasm and nucleus indicates that the mobility of GFP-sized proteins in both cellular compartments is approximately the same. Minor variations in the diffusional properties of GFP and other macromolecules in the cell nucleus relative to the cytoplasm have also been observed in other studies (Seksek et al., 1997; Houtsmuller et al., 1999; Phair and Mistelli, 2000). Note that although the similarity of the diffusion parameters in the nucleus and cytoplasm is evident, the underlying obstructing mechanisms for protein diffusion need not necessarily be the same.

GFP diffusion under different osmotic conditions

Generally, a change in cell volume invokes a different molecular concentration, that should affect the intracellular viscosity and hence the protein diffusion. To examine the relative influence of the intracellular concentration of solutes and proteins on the translational dynamics of soluble GFP molecules, cell volumes are manipulated by subjecting the *Dictyostelium* amoebae to different osmotic conditions. Due to the presence of a contractile vacuole dedicated to reduce the intracellular osmotic pressure under hypotonic conditions, wild-type *Dictyostelium* cells are able to survive

TABLE 1 Diffusion parameters, immobile fractions and effective viscosities as determined from the photobleaching experiments of GFP in *D. discoideum* under various conditions

Condition	Relative Volume	D ($\mu m^2/s$)	Immobile fraction (%)	η_{eff} (cP)
Free GFP		87 ± 2	0.0 ± 0.3	1.0
In Cells				
17 mM phosphate buffer	1.00 ± 0.15	24 ± 2	4.0 ± 0.3	3.63 ± 0.24
Distilled water	1.70 ± 0.19	46 ± 2	2.8 ± 0.3	1.89 ± 0.10
300 mM sorbitol	0.57 ± 0.10	17 ± 3	4.0 ± 0.3	5.11 ± 0.75
Lantrunculin-A	1.11 ± 0.7	42 ± 2	3.2 ± 0.3	2.07 ± 0.11
Nucleus		22 ± 2	4.0 ± 0.3	3.95 ± 0.28
In Polarized cells				1.05 ± 0.12
Front		33 ± 1	2.7 ± 0.3	2.63 ± 0.11
Middle		29 ± 2	2.8 ± 0.3	3.00 ± 0.19
Rear		33 ± 1	2.4 ± 0.3	2.63 ± 0.11

The error margins refer to the relative uncertainty of the fitting parameters.

in distilled water for more than an hour (Patterson, 1980; Nolta and Steck, 1994). Being suspended in distilled water, the average cell volume increases 1.7-fold with respect to a 17 mM phosphate-buffered medium. The increase in cell volume is accompanied by a rise of the intracellular GFP diffusion coefficient from 24 $\mu m^2/s$ to 46 $\mu m^2/s$, corresponding to a 1.9-fold increase in translational mobility (Table 1). Under these hypotonic conditions, an immobile fraction of fluorescent protein of 2.8% is observed. Alternatively, incubation in a hypertonic medium containing 300 mM sorbitol leads to a 1.8-fold reduction of the cell volume relative to the phosphate buffer. Correspondingly, the protein mobility is seen to decline. The photobleaching curve is best described by a diffusion constant of 17 $\mu m^2/s$ with an immobile contribution of 4.0% (Table 1).

GFP translational diffusion in polarized cells

Polarized *Dictyostelium* cells were subjected to photobleaching experiments to investigate the position-dependent diffusion of GFP. Due to the intrinsic refined spatial resolution of the spot photobleaching technique with subsequent confocal detection, molecular diffusion can be explored in different cellular domains. In these experiments, the laser beam was positioned at the front side of a migrating polar-

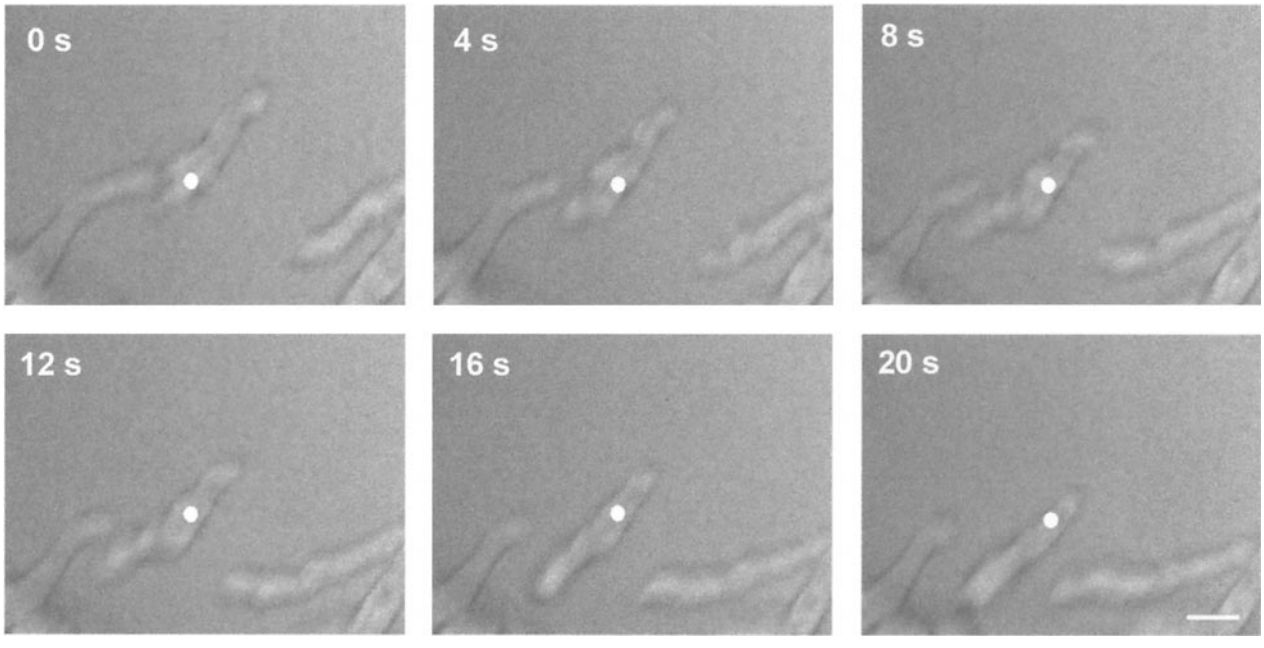

FIGURE 2 Mapping GFP diffusion as a function of position in highly locomotive polarized cells of *Dictyostelium*. Consecutive photobleaching measurements were conducted with 1-s intervals while polarized cells migrate through the focal spot. The bright dot designates the position of the laser beam. Scale bar measures 5 μm.

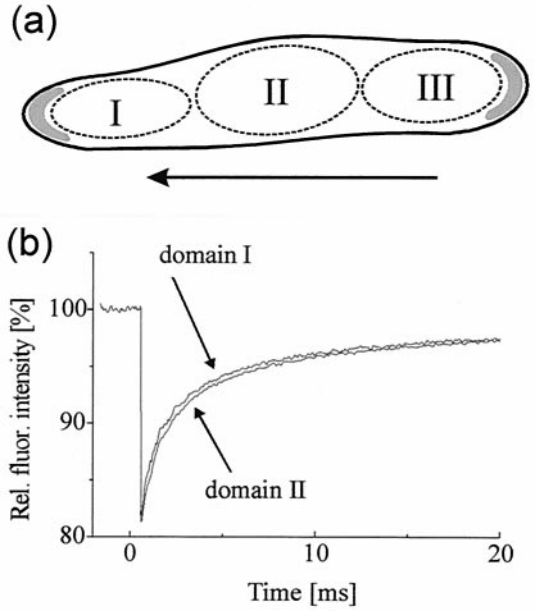

FIGURE 3 Molecular diffusion is a function of cellular domain in polarized amoebae. (*a*) Subdivision of cellular compartments as probed in the photobleaching experiments: I, anterior part; II, central part; and III, posterior domain of the cell. Shaded regions indicate accumulation zones of actin filaments. (*b*) Different diffusion coefficients are determined for the various compartments. In domain I the diffusion constant measures 29 $\mu m^2/s$, and in volume section II a molecular diffusion of 33 $\mu m^2/s$ is found. Average diffusion coefficients are calculated from 52 different cells.

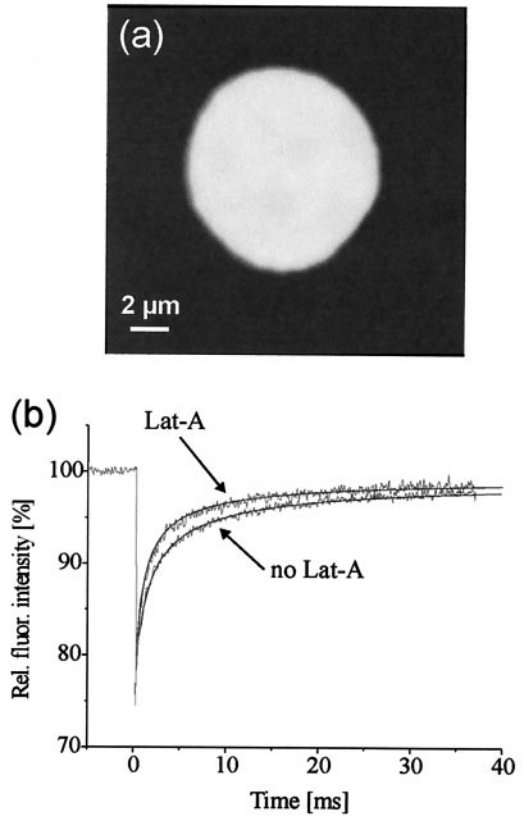

FIGURE 4 Mobility of GFP is enhanced in depolymerizing the actin cytoskeleton using Lat-A. (*a*) *Dictyostelium* cell 2 min after 1 μM Lat-A has been added to the cell suspension. All cells adopt a spherical morphology and active migration is depleted. A rather small volume increase of 10% is observed. (*b*) Photobleaching measurements 15 min after adding 1 μM Lat-A to the cells ($n = 48$). GFP diffusion coefficient measures 42 $\mu m^2/s$.

ized cell and subsequent photobleaching traces were recorded at 1-s intervals (Fig. 2). While the cell moves along a particular track, the laser beam position is kept fixed, leading to an array of position-specific photobleaching curves. Under the excitation conditions used, individual cells seem not to be affected by the FRAP illumination scheme and show regular chemotaxically driven migration during the time course of the measurement.

The intracellular GFP diffusion in polarized cells is faster than in nonpolarized cells. Additionally, a small difference is observed between different regions of the cell. Fig. 3 illustrates schematically in which domains of the cell molecular diffusion coefficients are determined. In the front part of the cell, GFP diffusion is characterized by a single diffusion constant with $D = 33 \pm 1$ $\mu m^2/s$. Within this volume fraction of the cell, organelle structures are largely depleted. Cellular organelles are predominantly assembled in the central region of the cell (Wessels and Soll, 1990) where the translational motions of GFP correspond to $D = 29 \pm 2$ $\mu m^2/s$. The density of membrane-bound structures in the rear part of the cell resembles that of the cell's leading face. In this domain, a diffusion constant of 33 ± 1 $\mu m^2/s$ is identified. Given the quality of the fit, we conclude that the difference in protein mobility observed in the different compartments of the cell is quantitatively significant (Table 1). The average immobile GFP population in polarized cells measures 2.6%, which is somewhat lower than in vegetative amoebae.

Actin cytoskeleton limits GFP mobility

To study the restrictions in protein mobility imposed mechanically by the actin cytoskeletal network, latrunculin-A (Lat-A) is used to inhibit the polymerized state of actin (Ayscough et al., 1998; Parent et al., 1998; Konzok et al., 1999). When Lat-A is added at a concentrations of 1 μM, *Dictyostelium* cells adopt a spherical shape after 2 min (Fig. 4). None of the cells showed active migration and the formation of pseudopodia was absent. We interpret these observations as being indicative of the disruption of the actin filamentous cytoskeleton. Contrary to yeast cells, which show a gradual increase in cell volume after addition of Lat-A, *Dictyostelium* cells do not swell considerably. The relative growth of cell volume is limited to 10%. The diffusion of GFP molecules in Lat-A-treated cells is substantially faster than in untreated cells. After 15 min of

incubation with 1 μM Lat-A, a diffusion constant of 42 $\mu m^2/s$ is deduced from the photobleaching data and the immobile fraction amounts to 3.2%. When the actin polymerization inhibitor is added at threefold higher concentration, no further increase of the GFP diffusion is observed. This indicates that at the present Lat-A concentrations virtually all the actin-related barriers for GFP mobility have been removed. Consistent with this observation, using rhodamine-phalloidin staining of filamentous actin it has been shown that the *Dictyostelium* actin network appears largely dissolved in cells treated with 1–5 μM Lat-A (Yuan and Chia, 2000; A. Yuan and C. P. Chia, University Nebraska-Lincoln, personal communication, 2001).

Because in Lat-A treated cells the influence of filamentous actin on the translational diffusive motions of GFP is absent, the mobility of the fluorescent protein is affected by the cellular medium and obstructions raised by organellar boundaries. To examine the nature of the non-actin effective viscositiy, we have measured GFP diffusion on varying the cell volume. When the volume of the cell is changed in the presence of Lat-A, the intracellular viscosity is seen to vary in an almost linear fashion with the concentration of intracellular constituents (Fig. 5 *a*). The solid line in Fig. 5 refers to a least-squares fit to the experimental data points using the function $\eta = 1 + c(V_0/V)^b$, which is based on Eq. 8. Here we have allowed for a nonlinear b to account for subtle deviations from pure solvent-like behavior of the viscosity. In case the change in cellular viscosity can be fully attributed to the liquid cell medium, the variable b assumes the value 1. However, the fitting procedure reveals that $b = 1.3$, which represents a small divergence from an ideal solvent response (dashed line). The slight nonlinearity of the non-actin-like cellular viscosity can be explained by the presence of obstacles for protein motion as introduced by membrane surfaces and macromolecular structures.

From the established relation between the cell's volume and non-actin-related protein diffusion in Lat-A-treated cells (Fig. 5 *a*), an internal viscosity ($\eta_{med} + \kappa_{other}$) of 2.2 cP can be allocated in vegetative *Dictyostelium* cells at room temperature. Against this background, the actin cytoskeletal network contributes a mechanically motional impediment of GFP-sized molecules. In comparing GFP diffusion in cells that have been exposed to Lat-A with protein mobility in untreated vegetative cells, it can be calculated that κ_{actin} amounts to 1.4 cP.

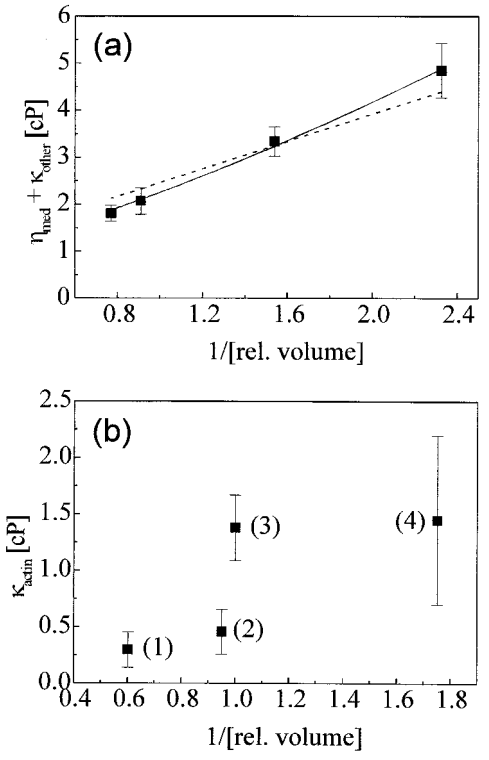

FIGURE 5 Variation of the viscosity with the concentration of intracellular constituents ($\propto 1/V$). (*a*) Intracellular viscosity in the absence of the actin cytoskeleton. Measurements are performed in Lat-A-treated amoebae at room temperature, and cell volumes are manipulated by changing the osmolarity of the buffer. Solid line corresponds to a least-squares fitting of the data points allowing for a nonlinearity in the response of the intracellular domain according to $\eta = 1 + c(V_0/V)^b$ with $b = 1.3$ and $c = 1.2$. The dashed line refers to a fit based on a solvent-like behavior of the viscosity, which applies when $b = 1.0$. (*b*) Calculated contributions of the effective viscosity enforced by the actin filamentous network for the various conditions examined: (1) cells in distilled water, (2) polarized cells (domain I), (3) cells in 17 mM phosphate buffer, and (4) cells in 300 mM sorbitol buffer solution. Values are calculated from measured diffusion coefficients and the cell volume dependence as determined from the fit in *a*.

Motional restrictions of GFP depend on distribution of the actin network

In Table 1 we summarize our findings of the GFP diffusion measurements in *Dictyostelium* cells. In making use of Fig. 5 *a* and Eqs. 7 and 8, the obstructing effect of the actin filaments can be distinguished in each of the cellular conditions examined. The effect of actin-induced restrictions shows a dependence on the physiological circumstances. For cells suspended in distilled water the actin-blocking activity leads to an effective viscosity $\kappa_{actin} = 0.27 \pm 0.16$ cP whereas in cells immersed in the hypertonic buffer the obstructing effects account for 1.46 ± 0.71 cP. In polarized cells the actin-blocking activity differs from that in vegetative cells as well. In the anterior and posterior domains of the cell κ_{actin} can be computed as 0.46 ± 0.20 cP. In Fig. 5 *b*, the effect of the actin cytoskeleton on GFP mobility is plotted as a function of the relative cell volume. Contrary to the remaining mechanisms that constitute the viscous environment of the GFP molecules, the actin impediment does not show a correlation with the cellular volume. Rather, the blocking activity is connected to a particular distribution of the actin filaments associated with a specific intracellular condition.

DISCUSSION

Soluble GFP is a reliable probe for intracellular protein diffusion

In this study photobleaching measurements were performed to investigate physical barriers that constraint protein translational diffusion. The extracted diffusion constants and related physical parameters depend on the reliability of GFP as a representative probe for protein diffusion. A particular advantage of using GFP as the target molecule is that its expression in the cell results in a homogeneous staining of the cellular aqueous domains, which facilitates the practical application of the photobleaching technique. Concentration levels of GFP generally did not exceed 1.0 μM so that dimerization or putative crystallization of the fluorophore can be ruled out. Still, a number of factors might influence the accuracy of the photobleaching experiments. A significant fraction of reversibly bleached GFP molecules may interfere with the recovery kinetics of the irreversibly bleached population. It is known that various mutants of the GFP molecule can undergo excitation-intensity-dependent photoconversions that relate to blinking of the emissive response (Garcia-Parajo et al., 2000; Schwille et al., 2000; Jung et al., 2000). Under the present conditions, no signs of reversible components were identified in the dynamics of the fluorescence recovery in *Dictyostelium* cells. Also, an appreciable amount of nonspecific binding of the probe molecule may perturb the recovery dynamics. The GFP molecule is, however, remarkably inert, and no significant binding interactions with intracellular compounds that affect the photobleaching measurements have been reported so far.

Under the benign excitation conditions employed, possible photothermal effects that find their repercussion in cellular functioning have not been observed. In particular, highly locomotive cells seem not to be affected by the laser radiation applied. Therefore, we surmise that the molecular diffusional properties of intracellular compounds are not altered due to the incident light and represent the native situation in *Dictyostelium* cells.

Under the various conditions examined, the fluorescence recovery is excellently described with a single diffusion coefficient. This observation suggests that the affected diffusion can be correlated to an effective intracellular viscosity as exemplified by Eq. 7. Although the actual recovery process may be composed of multicomponent diffusion mechanisms (Periasamy and Verkman, 1998), a single effective viscosity suffices to describe the sampled data with a high accuracy. As η_{eff} covers both the effects of the cellular medium and the impediment connected with collisional interactions, the observed single diffusive component strengthens the assumption that the actin-induced and organelle-related limitations in protein mobility can be reliably modeled by the viscosity-like parameter κ.

A moderate discrepancy with the predicted fluorescence recovery based on a single diffusion coefficient is observed in cells exposed to hypertonic surroundings. Especially at longer times, a small additional contribution ($\sim$10%) reminiscent of a slow diffusion component ($\sim$3 $\mu m^2/s$) is recognized. These altered diffusional dynamics indicate that the close packing of intracellular constituents associated with the reduced cell volume introduce new diffusional pathways of GFP-sized molecular compounds. The more rapidly diffusing fraction ($\sim$90%) is adequately described with a diffusion constant of 17 $\mu m^2/s$.

Filamentous actin constitutes a primary barrier for protein diffusion

In a dilute aqueous solution at room temperature, a protein such as GFP experiences an environmental viscosity of 1.0 cP. Clearly, in the interior of living cells protein diffusion differs significantly from diffusion in a simple solution. In amoebae of *Dictyostelium*, the intracellular viscosity as determined from the GFP FRAP measurements amounts to 3.6 cP. This supplementary increase of 2.6 cP relative to water is characterized by the added restrained mobility of the probe molecule, enforced by the high intracellular molecular concentration and by mechanical barriers.

On Lat-A-induced depolymerization of the actin filamentous network, an important source of mechanical obstructions for protein mobility in the cytoplasm is removed. In vegetative cells, the intracellular viscosity decreases to 2.2 cP in dousing the filamentous form of actin. From these numbers, the viscous contribution of the actin network can be determined as 1.4 cP. The three-dimensional network of actin filaments explains 53% of the restricted translational motions of the probe molecule. The remaining 47% (1.2 cP) restricted translational motion is caused by the increased viscosity of the cytosolic liquid and by mechanical obstruction attributable to organelles. Taking into account these additional effects of the cellular medium, it can be ascertained that filamentous actin comprises the major mechanical barrier for GFP diffusion.

Contribution of non-actin barriers to reduced GFP diffusion

Large variations are found in the protein's diffusional mobility when the cellular conditions are changed. Obviously, the effective viscosity changes when the rheological conditions change in response to altered environmental conditions. Generally, when a uniform distribution of molecular compounds is hypothesized, any change in intracellular molecular concentration is, according to Eq. 8, accompanied by a corresponding change of the viscosity. In the absence of polymerized actin,

such a trend is indeed observed. As displayed in Fig. 5 *a*, the almost linear relationship between the intracellular concentration and the viscosity observed suggests that the viscous properties of the intracellular environment predominantly show a solvent-like behavior. In extrapolating the data points in Fig. 5 *a*, one obtains a reliable estimate of the contribution of the non-actin-related viscosity in each of the conditions examined. In cells immersed in distilled water for instance, the conjoint viscosity determined by η_{med} and κ_{other} measures 1.6 cP whereas this contribution increases to 3.6 cP in cells exposed to 300 mM sorbitol. As such, the change in intracellular concentration provides the basis of the global trends of the effective viscosity discerned under the different osmotic conditions (Table 1).

In polarized amoebae of *Dictyostelium*, the strong morphological modifications are not coupled to a change in cellular volume. This suggests that the total cell volume is mainly dictated by the osmolarity of the non-nutrient phosphate buffer. Consequently, the observed facilitated translational mobility of the GFP molecule in polarized cells cannot be ascribed to a reduced viscosity of the cell medium. Rather, a variation in the mechanical restrictions for diffusion seems to be responsible for the enhanced translational motion of GFP.

Different diffusion coefficients are found in different domains of the polarized cells. In particular, in the cell's central region the GFP molecule appears to be slightly more hindered in its translational motions than in the extended front and rear domains of the cell. Both a different organization of actin filaments or a compartment-dependent concentration of organellar barriers can account for the observed difference. If it is assumed that the distinction is solely due to an agglomeration of membrane-bound structures in the middle part of the cell, we may estimate that organelle accumulation brings about a 10% change in protein mobility. This number might be even lower, if one considers the supporting role the actin filaments play in organelle localization (Luby-Phelps et al., 1987), giving rise to a possibly more condensed actin network in the central region of the cell. Accordingly, collisional interactions with membranes and spatial confinement due to congregation of macro-sized structures introduce only a moderate hampering of GFP diffusion. This finding is supported by recent Monte Carlo simulations of molecular diffusion in the aqueous lumen of organelles, in which seriously hindered diffusion was observed only for appallingly high organellar barriers (Ölveczky and Verkman, 1998). The modest impact of organellar structures on protein diffusion agrees furthermore with the perception of a solvent-like behavior of the viscosity that is uncommitted to the cytoskeleton.

Protein diffusion shows a conditional dependence on the density of the actin network

Next to the variation in the concentration-related viscosity, a varying contribution of the actin-induced viscosity is seen under the various conditions studied. Contrary to the joint viscosity of the cell medium and κ_{other}, a straightforward relationship between a changing cell volume and the actin blocking activity cannot be established (Fig. 5 *b*). Instead, the contribution of κ to molecular mobility correlates with a condition-specific distribution and condensation of actin filaments. In cells that shrink under the influence of hypertonicity, for instance, the actin-related obstructions in the bulk of the cell are approximately the same as in cells under less stringent osmotic conditions. This perception conflicts with a model that assumes a uniform scaling of the actin network with cell volume. In the latter situation a compression of actin fibers associated with squeezed intra-filamentous apertures would lead to a considerable rise of the mechanical blocking activity. In this regard, a putative reorganization of the actin filaments seems more likely to explain our data. As was previously shown, actin is seen to accumulate in cortical regions in response to hypertonic surroundings, leaving a less dense network in the central regions of the cell (Kuwayama et al., 1996; Zischka et al., 1999). Our results harmonize with that view.

A similar reasoning accounts for the limited obstructed protein diffusion that can be assigned to the actin filaments in polarized cells. Our results coincide with models that confer actin filaments a fundamental role in cell locomotive behavior (Condeelis, 1993). Due to agglomeration of filamentous actin near the cell edges (Yumura and Fukui, 1998; Ming Pang et al., 1998; Novak and Titus, 1997), actin-induced motional hindrance reduces to 0.46 cP throughout the bulk of the cell's interior. The thinning of the actin cytoskeleton brings about an intracellular environment in which diffusion-limited transport is enhanced by a factor of 1.4. Hence, the rheological conditions of the cell cytoplasm in polarized *Dictyostelium* cells allow more rapid enzymatic kinetics, which possibly contribute to rectified motility and enhanced intracellular communication. Conversely, based on our results we may speculate that the protein diffusion is substantially encumbered in the cortical domains with higher filamentous actin concentration. This latter feature may have important implications for protein-mediated information exchange from the cellular rim to the interior parts of the cell.

The filament-induced obstructions are primarily collisional in nature. Severe limitation due to spatial confinement and cage formation is not supported by the photobleaching measurements. This can be inferred from the observation that not much diversity is assessed in the immobile fraction of the bleached GFP population when the cellular conditions are varied. In cells free from polymerized actin, the immobile fraction is seen to decrease only modestly relative to cells possessing an intact cytoskeletal network. Nevertheless, a certain correlation can be recognized between the degree of protein immobilization and the density of actin filaments in the probed regions. This suggests that a small percentage of the

GFP molecules is captured in the meshes of the actin network. In this case, the residence times of these molecules in actin-formed micro-compartments are at least three orders of magnitude longer than the recovery times of the photobleaching curves in our experiments.

The present study shows that the mobility of GFP-sized proteins is strongly dependent on the organizational details of the actin filamentous network. Because protein translational motions are directly coupled to the rate of diffusion-limited biochemical reactions, the dynamic distribution of the actin cytoskeleton may influence the intracellular kinetics to a certain extent. In this regard, any modeling of cellular reaction dynamics should anticipate the spatially varying organization of the actin cytoskeleton.

REFERENCES

Axelrod, D., D. E. Koppel, J. Schlessinger, E. Elson, and W. W. Webb. 1976. Mobility measurement by analysis of fluorescence photobleaching recovery. *Biophys. J.* 16:1055–1069.

Ayscough, K. R., J. Stryker, N. Pokala, M. Sanders, P. Crews, and D. G. Drubin. 1997. High rates of filament turnover in budding yeast and roles for actin in establishment and maintenance of cell polarity revealed using the actin inhibitor latrunculin-A. *J. Cell. Biol.* 137: 399–416.

Blonk, J. C. G., A. Don, H. van Aalst, and J. J. Birmingham. 1993. Fluorescence photobleaching recovery in the confocal scanning microscope. *J. Microsc.* 169:363–374.

Bray, D., and C. Thomas. 1975. The actin content of fibroblasts. *Biochem. J.* 147:221–228.

Brinkman, H. C. 1947. A calculation of the viscous force exerted by a flowing fluid in a dense swarm of particles. *Appl. Sci. Res. A.* 1:27–34.

Brown, E. B., E. Shinn Wu, W. Zipfel, and W. W. Webb. 1999. Measurement of molecular diffusion in solution by multiphoton fluorescence photobleaching recovery. *Biophys. J.* 77:2837–2849.

Condeelis, J. 1993. Life at the leading edge: the formation of cell protrusions. *Annu. Rev. Cell Biol.* 9:411–444.

Cooper, J. A. 1991. The role of actin polymerization in cell motility. *Annu. Rev. Physiol.* 53:585–605.

Fishkind, D. J., and Y. L. Wang. 1995. New horizon for cytokinesis. *Curr. Opin. Cell. Biol*: 7:23–31.

Garcia-Parajo, M. F., G. M. J. Segers-Nolten, J. A. Veerman, J. Greve, and N. F. van Hulst. 2000. Real-time light-driven dynamics of the fluorescence emission in single green fluorescent protein molecules. *Proc. Natl. Acad. Sci. U.S.A.* 97:7237–7242.

Houtsmuller, A. B., S. Rademakers, A. L. Nigg, D. Hoogstraten, J. H. J. Hoeijmakers, and W. Vermeulen. 1999. Action of DNA repair endonuclease ERCC1/XPF in living cells. *Science.* 284:958–961.

Johansson, L., and J. E. Löfroth. 1993. Diffusion and interaction in gels and solutions. IV. Hard sphere Brownian dynamics simulations, *J. Chem. Phys.* 98:7471–7479.

Johnson, E. M., D. A. Berk, K. J. Jain, and W. M. Deen. 1996. Hindered diffusion in agarose gels: test of effective medium model. *Biophys. J.* 70:1017–1026.

Jung, G., S. Mais, A. Zumbusch, and C. Bräuchle. 2000. The role of dark states in the photodynamics of the green fluorescent protein examined with two-colour fluorescence correlation spectroscopy. *J. Phys. Chem. A* 104:873–876.

Konzok, A., I. Weber, E. Simmeth, U. Hacker, M. Maniak, and A. Müller-Taubenberger. 1999. Daip1, a *Dictyostelium* homologue of the yeast actin-interacting protein 1, is involved in endocytosis, cytokinesis and motility. *J. Cell. Biol*. 146:453–464.

Kuwayama, H., M. Ecke, G. Gerisch, and P. J. M. van Haastert. 1996. Protection against osmotic stress by cGMP mediated myosin phosphorylation. *Science.* 271:207–209.

Luby-Phelps, K. 2000. Cytoarchitecture and physical properties of the cytoplasm: volume, viscosity, diffusion, intracellular surface area. *Int. Rev. Cytol.*189–221.

Luby-Phelps, K., E. P. Castle, D. L. Taylor, and F. Lanni. 1987. Hindered diffusion of inert tracer particles in the cytoplasm of mouse 3T3 cells, *Proc. Natl. Acad. Sci. U.S.A.* 84:4910–4913.

Luby-Phelps, K., D. L. Taylor, and F. Lanni. 1986. Probing the structure of cytoplasm. *J. Cell. Biol.* 102:2015–2022.

Ming Pang, K., U. Lee, and D. A. Knecht. 1998. Use of a fusion protein between GFP and an actin-binding domain to visualize transient filamentous-actin structures. *Curr. Biol.* 8:405–408.

Nolta, K. V., and T. L. Steck. 1994. Isolation and initial characterization of the bipartite contractile vacuole complex from *Dictyostelium discoideum*. *J. Biol. Chem.* 269:2225–2233.

Novak, K. D., and M. A. Titus. 1997. Myosin I overexpression impairs cell migration. *J. Cell Biol.* 136:633–647.

Ölveczky, B. P., and A. S. Verkman. 1998. Monte Carlo analysis of obstructed diffusion in three dimensions: application to molecular diffusion in organelles. *Biophys. J.* 74:2722–2730.

Parent, C. A., B. J. Blacklock, W. M. Frölich, D. B. Douglas, and P. N. Devreotes. 1998. G protein signaling events are activated at the leading edge of chemotactic cells. *Cell.* 95:91–91.

Patterson, D. J. 1980. Contractile vacuoles and associated structures: their organization and function. *Biol. Rev.* 55:1–46.

Periasamy, N., and A. S. Verkman. 1998. Analysis of fluorophore diffusion by continuous distributions of diffusion coefficients: application to photobleaching measurements of multicomponent and anomalous diffusion. *Biophys. J.* 75:557–567.

Phair, R., and T. Mistelli. 2000. High mobility of proteins in the mammalian cell nucleus. *Science.* 404:604–609.

Popov, S., and M. M. Po. 1992. Diffusional transport of macromolecules in developing nerve processes. *J. Neurosci.* 12:77–85.

Schwille, P., S. Kummer, A. A. Heikal, W. E. Moerner, and W. W. Webb. 2000. Fluorescence correlation spectroscopy reveals fast optical excitation-driven intramolecular dynamics of yellow fluorescent proteins. *Proc. Natl. Acad. Sci. U.S.A.* 97:151–156.

Seksek, O., J. Biwersi, and A. S. Verkman. 1997. Translational diffusion of macromolecule-sized solutes in cytoplasm and nucleus. *J. Cell Biol.* 138:131–142.

Spudich, J. A. 1987. *Dictyostelium discoideum*: molecular approaches to cell biology. *Methods Cell. Biol.* 28:1–516.

Swaminathan, R., C. P. Hoang, and A. S. Verkman. 1997. Photobleaching recovery and anisotropy decay of green fluorescent protein GFP-S65T in solution in cells: cytoplasmic viscosity probed by green fluorescent protein translational and rotational motion. *Biophys. J.* 72:1900–1907.

Terry, B. R., E. K. Mattews, and J. Haselhoff. 1995. Molecular characteristics of recombinant green fluorescent protein by fluorescence correlation spectroscopy. *Biochem. Biophys. Res. Commun*. 217: 21–27.

Wessels, D., and D. R. Soll. 1990. Myosin II heavy chain null mutant of *Dictyostelium* exhibits defective intracellular particle movement. *J. Cell Biol.* 111:1137–1148.

Yuan, A., and C. P. Chia. 2000. Integrity of the actin cytoskeleton required for both phagocytosis and macropinocytosis in *Dictyostelium discoideum*. *Mol. Biol. Cell.* 11:376a.

Yumura, S., and Y. Fukui. 1998. Spatiotemporal dynamics of actin concentration during cytokinesis and locomotion in *Dictyostelium. J. Cell Sci.* 111:2097–2108.

Zischka, H., F. Oehme, T. Pintsch, A. Ott, H. Keller, J. Kellerman, and S. C. Schuster. 1999. Rearrangement of cortex proteins constitutes an osmoprotective mechanism in *Dictyostelium*. *EMBO J.* 18: 4241–4249.